Supporting Information for

Metal-Oleate Complex Derived Bimetallic Oxides Nanoparticles Encapsulated in 3D Graphene Networks as Anodes for Efficient Lithium Storage with Pseudocapacitance

Yingying Cao[1, #], Kaiming Geng[1, #], Hongbo Geng[2, *], Huixiang Ang[3], Jie Pei[1], Yayuan Liu[1], Xueqin Cao[1], Junwei Zheng[4], Hongwei Gu[1, *]

[1]Key Laboratory of Organic Synthesis of Jiangsu Province, College of Chemistry, Chemical Engineering and Materials Science and Collaborative Innovation Center of Suzhou Nano Science and Technology, Soochow University, Suzhou 215123, People's Republic of China

[2]School of Chemical Engineering and Light Industry, Guangdong University of Technology, Guangzhou 510006, People's Republic of China

[3]School of Chemical and Biomedical Engineering, Nanyang Technological University, Singapore 637459, Singapore

[4]College of Physics, Optoelectronic and Energy, Soochow University, Suzhou 215006, People's Republic of China

[#]These authors contributed equally to this work

*Corresponding authors. E-mail: hongwei@suda.edu.cn (Hongwei Gu); hbgeng@gdut.edu.cn (Hongbo Geng)

Supplementary Figures and Tables

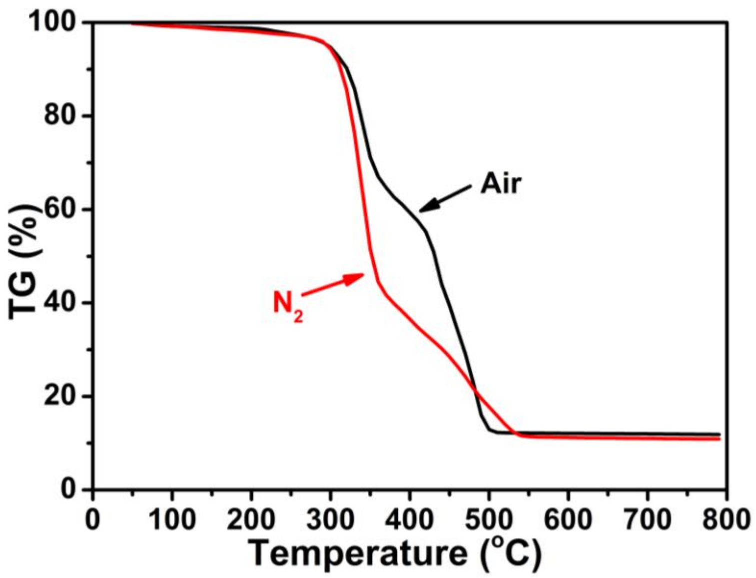

Fig. S1 TGA plot of the metal-oleate complex precursor under N_2 and air atmospheres

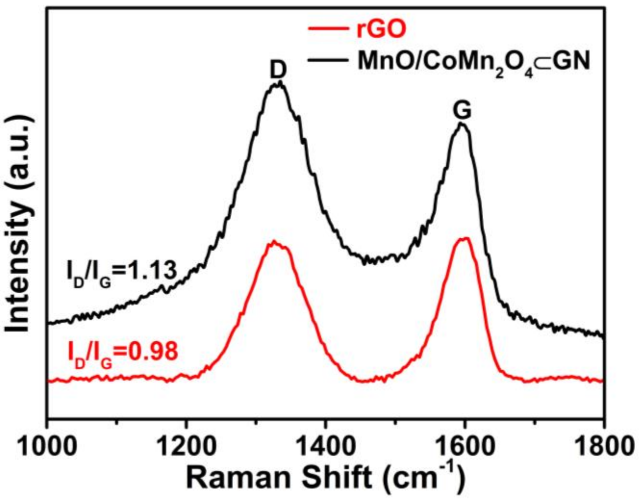

Fig. S2 Raman spectra of $MnO/CoMn_2O_4{\subset}GN$ and rGO

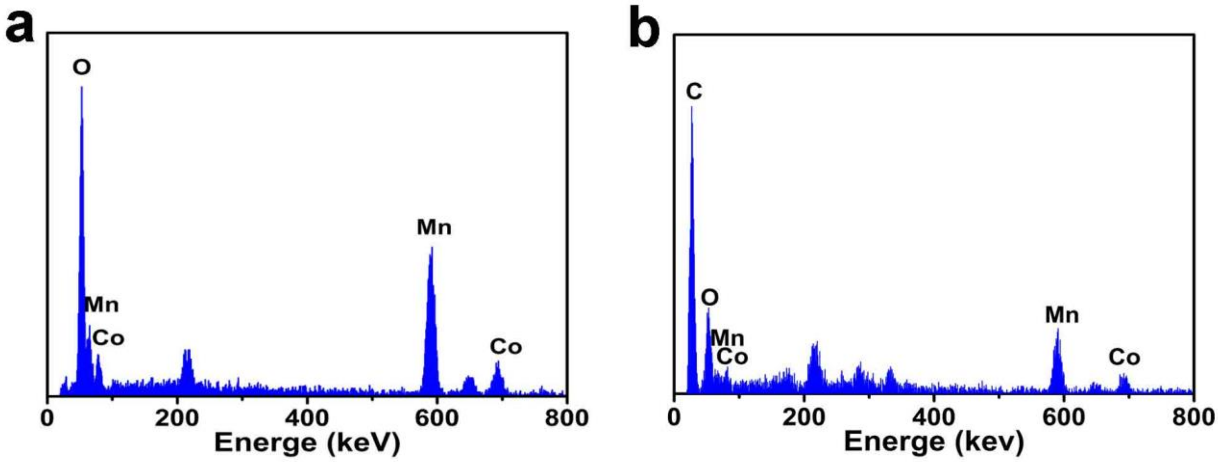

Fig. S3 Energy-dispersive X-ray spectroscopy (EDS) plots of $CoMn_2O_4$ and $MnO/CoMn_2O_4{\subset}GN$

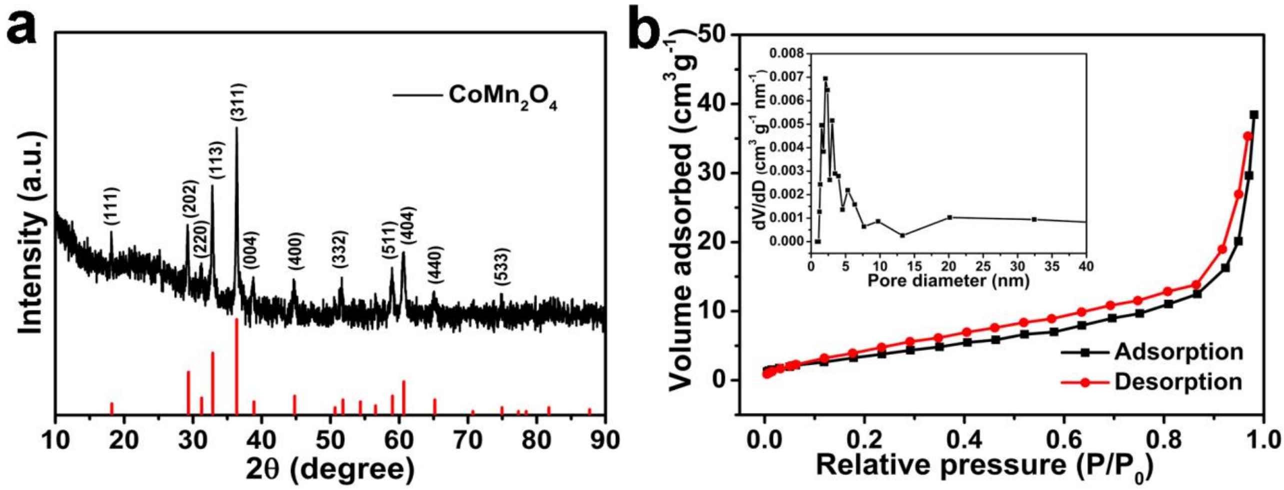

Fig. S4 a XRD pattern of the $CoMn_2O_4$. **b** Nitrogen adsorption-desorption isotherms and the pore size distribution curve of the $CoMn_2O_4$

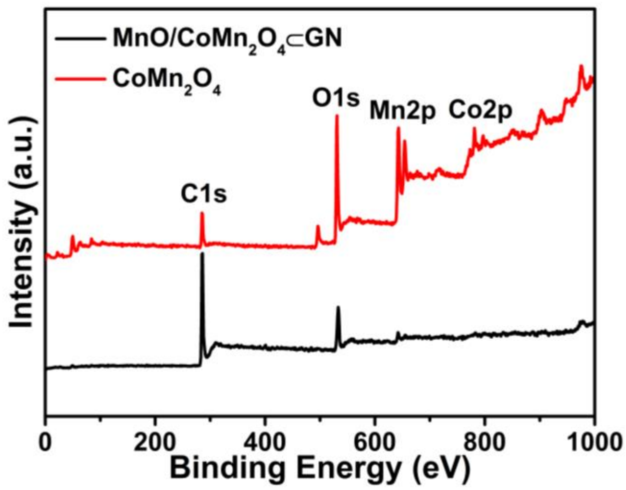

Fig. S5 XPS spectra of the $CoMn_2O_4$ and $MnO/CoMn_2O_4 \subset GN$ samples

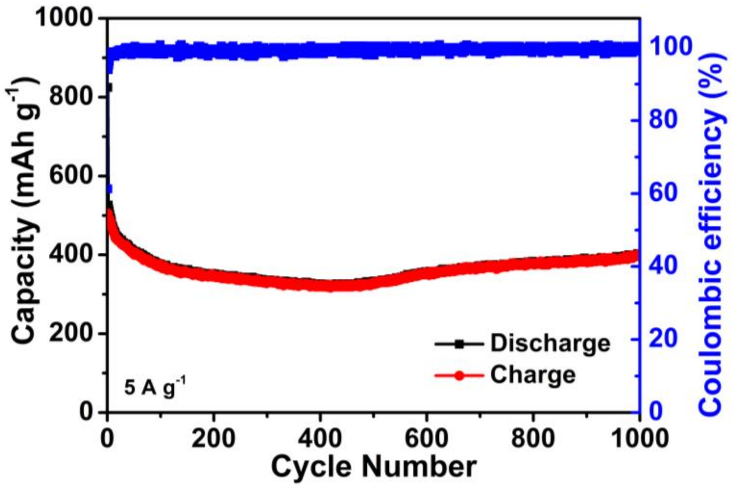

Fig. S6 Cycling performance and coulombic efficiency of $MnO/CoMn_2O_4 \subset GN$ at a current density of 5 A g^{-1}

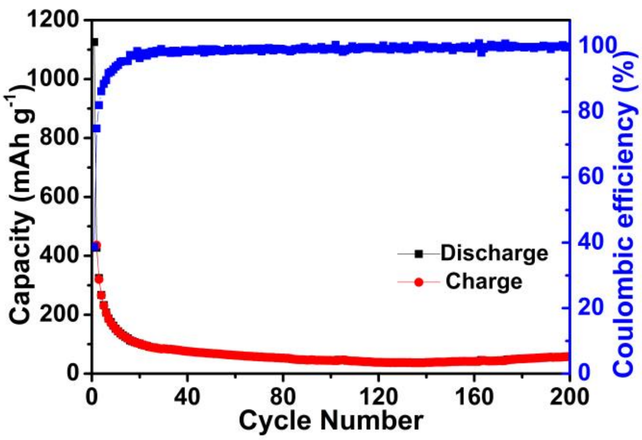

Fig. S7 Cycling performance and coulombic efficiency of pure $CoMn_2O_4$ at a current density of 0.1 A g^{-1}

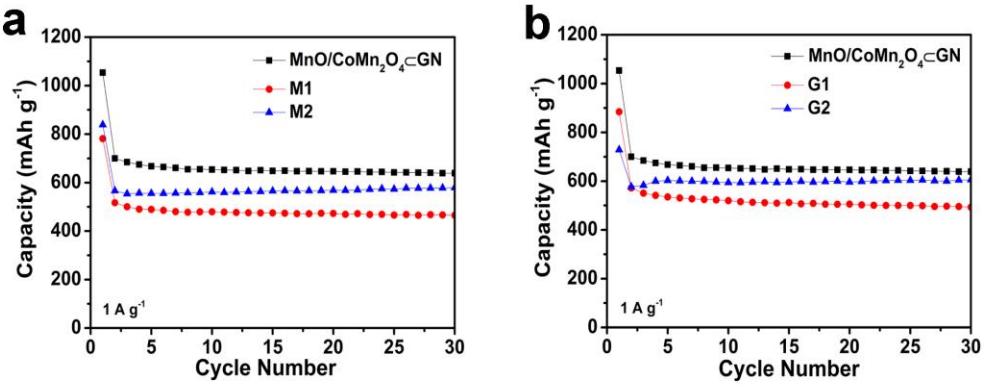

Fig. S8 Cycling performances of MnO/CoMn$_2$O$_4$⊂GN, M1, M2, G1, and G2 at a current density of 1 A g^{-1}

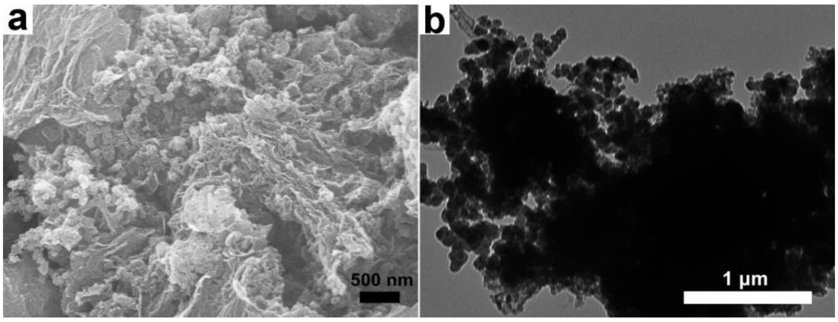

Fig. S9 a SEM and **b** TEM images of MnO/CoMn$_2$O$_4$⊂GN after 150 cycles at 0.1 A g^{-1}

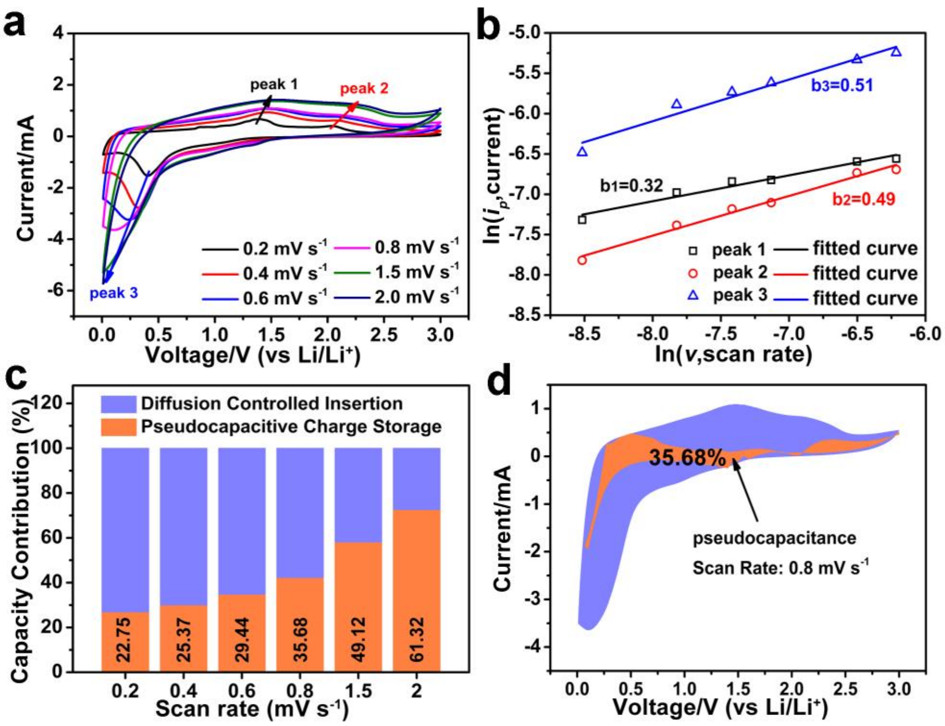

Fig. S10 a CV profiles of the pure CoMn$_2$O$_4$ electrodes at different scan rates with the potential range between 0.01 and 3.0 V. **b** The fitted lines and ln(i_p) *versus* ln(v) plots at different oxidation and reduction states. **c** The percentages of pseudocapacitive contribution at different scan rates. **d** Pseudocapacitive (red) and diffusion-controlled (blue) contribution to the charge storage of CoMn$_2$O$_4$ at 0.8 mV s^{-1}

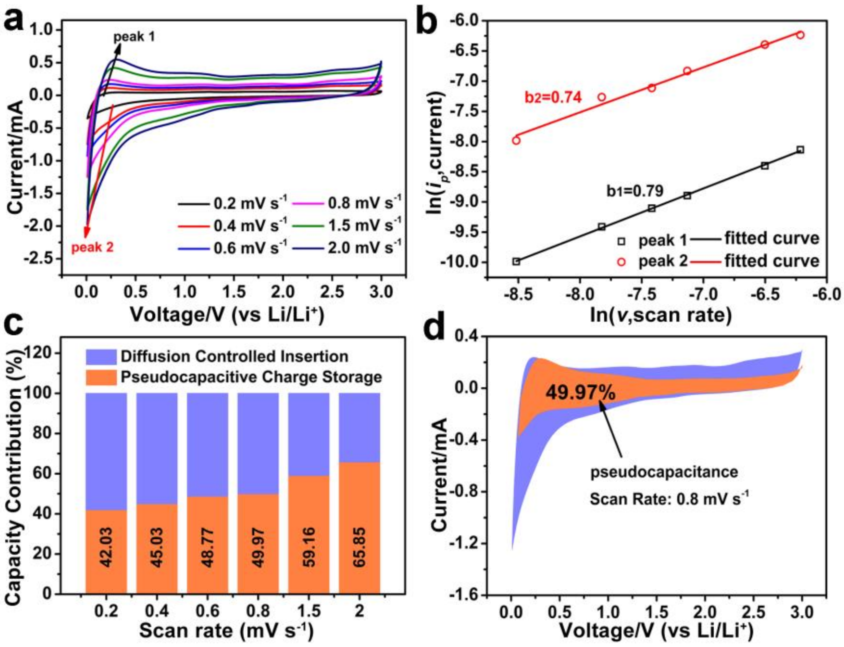

Fig. S11 a CV profiles of the rGO electrodes at different scan rates with the potential range between 0.01 and 3.0 V. **b** The fitted lines and ln(i_p) *versus* ln(v) plots at different oxidation and reduction states. **c** The percentages of pseudocapacitive contribution at different scan rates. **d** Pseudocapacitive (red) and diffusion-controlled (blue) contribution to the charge storage of rGO at 0.8 mV s^{-1}

Table S1 The feed ratio of M1, M2, G1, and G2

	$CoCl_2 \cdot 6H_2O$ (mmol)	$MnCl_2 \cdot 4H_2O$ (mmol)	GO (mg)
$MnO/CoMn_2O_4 \subset GN$	3.0	9.0	40
M1	1.5	9.0	40
M2	3.0	4.5	40
G1	3.0	9.0	80
G2	3.0	9.0	20

Table S2 The content of each component of $CoMn_2O_4$

Element	Co K	Mn K	O K	Total
Wt%	20.61	56.99	22.40	100

Table S3 The content of each component of $MnO/CoMn_2O_4 \subset GN$

Element	Co K	Mn K	O K	C K	Total
Wt%	9.33	20.4	14.29	55.98	100